Effects of ALDH2 gene expression on the oxidative stress-mediated NF-κB/mTOR pathway in ketamine-induced cystitis

XIAO JIAN XI*, YONG YAO*, PENG GU and MIN HAO ZHANG

Department of Urology, Wuxi Xishan People's Hospital, Wuxi, Jiangsu 214105, P.R. China

Received October 7, 2025; Accepted February 25, 2026

DOI: 10.3892/mmr.2026.13895

Abstract. Aldehyde dehydrogenase 2 (ALDH2) serves an important role in regulating the development of organ injury. The present study aimed to investigate the effects of ALDH2 gene expression on the oxidative stress-mediated NF-κB/mTOR pathway in ketamine (Ket)-induced cystitis (KIC). Primarily, human bladder epithelial cells of the SV-HUC-1 cell line were divided into groups for incubation with different concentrations of Ket: 0, 0.5, 1, 1.5 and 2 mM. ALDH2 protein expression was then detected after 48 h of incubation with Ket. Subsequently, SV-HUC-1 cells were separated into a number of treatment groups, including: i) Control groups, comprising negative control (NC), NC + mTOR activator MHY1485 (Act), NC + Ket and NC + Ket + Act groups; ii) ALDH2 knockdown groups that were transfected with siRNA sequences targeting ALDH2 (si-ALDH2), including si-ALDH2, si-ALDH2 + Act, si-ALDH2 + Ket and si-ALDH2 + Ket + Act groups; and iii) ALDH2 overexpression (OE-ALDH2) transfection groups, comprising OE-ALDH2, OE-ALDH2 + Act, OE-ALDH2 + Ket and OE-ALDH2 + Ket + Act groups. The levels of apoptosis, oxidative stress and inflammatory protein expression were assessed in each group. The results of the present study demonstrated that ALDH2 protein expression was significantly higher after treatment with Ket compared with the control group. Further analysis revealed that the si-ALDH2 + Ket group demonstrated the highest levels of apoptosis, oxidative stress and inflammatory protein expression amongst all treatment groups. The levels of these indicators notably improved in the OE-ALDH2 + Ket group compared with the NC + Ket group. Therefore, the results of the present study revealed that ALDH2 overexpression reduced Ket-induced apoptosis, oxidative stress and inflammatory protein expression. Furthermore, co-treatment with Act was shown to mitigate these factors. Additionally, ALDH2 may have modulated the inflammatory response by promoting mTOR activation and inhibiting NF-κB phosphorylation. The present study concluded that ALDH2 may represent a novel target for KIC treatment.

Correspondence to: Dr Min Hao Zhang, Department of Urology, Wuxi Xishan People's Hospital, 1128 Dacheng Road, Xishan, Wuxi, Jiangsu 214105, P.R. China
E-mail: zmhjj1981@163.com

*Contributed equally

Key words: ketamine-induced cystitis, aldehyde dehydrogenase 2, oxidative stress, mTOR, NF-κB

Introduction

Ketamine (Ket), commonly known as K powder, induces a strong sense of euphoria and exhibits notable hallucinogenic properties, leading to a large number of individuals, predominantly young individuals, that misuse this substance for recreational purposes (1). Studies have identified that long-term Ket abuse can cause damage to the nervous (2), cardiovascular (3) and urinary systems (4). The most common complications of urinary system damage are categorized as lower urinary tract symptoms (LUTS), characterized by frequent urination, urgency, suprapubic discomfort and hematuria. Symptoms of Ket usage that bear similarity to interstitial cystitis are attributed to Ket-induced cystitis (KIC) (5); however, the pathogenesis of this condition remains ambiguous. Previous studies suggest that Ket and its metabolites in urine exert direct toxic effects on bladder urothelial cells, resulting in chronic inflammation and fibrosis of the bladder mucosa (6,7).

Aldehyde dehydrogenase 2 (ALDH2) is an important enzyme in aldehyde metabolism and plays an important role in antioxidant protection (8). Studies have revealed that inhibiting ALDH2 expression can promote the inflammatory response in septic rats, thereby aggravating kidney damage (9,10). ALDH2 activation can also mitigate the hepatotoxic effects of acetaminophen and mediate cell damage caused by resultant oxidative products (11). Additionally, ALDH2 may exert protective effects against myocardial damage associated with pulmonary hypertension (12). These findings suggest that ALDH2 plays an important role in mediating oxidative stress and regulating inflammation during the consequent organ damage. Previous studies have revealed that ALDH2 expression is closely associated with urinary system diseases; ALDH2 has demonstrated anti-inflammatory protective effects in diseases such as renal ischemia-reperfusion injury (13), acute pyelitis (14), LUTS (15) and bladder tumors (16).

Our previous study identified that ALDH2 is upregulated in mice following Ket administration and that ALDH2 deficiency in mice aggravates KIC (17). However, the effects of ALDH2 on KIC *in vitro* remain to be fully elucidated. While

our previous investigation on ALDH2 knockout mice demonstrated that ALDH2 deficiency exacerbated KIC pathology, the specific cellular mechanisms and signaling pathways involved remain undefined. Previous studies have also indicated that ALDH2 mitigates lipopolysaccharide-induced damage to myocardial H9C2 cells through the cyclic GMP-AMP synthase/stimulator of interferon genes protein pathway (18) and protects against acute kidney injury via autophagy regulation in HK-2 cells (19). The present study aimed to elucidate the molecular mechanisms through which ALDH2 protected bladder epithelial cells from Ket-induced injury, specifically by examining the oxidative stress-mediated crosstalk between the NF-κB and mTOR pathways.

Materials and methods

Cell culture and reagents. The immortalized human bladder epithelial cell line SV-HUC-1 was purchased from The Cell Bank of Type Culture Collection of The Chinese Academy of Sciences. Cells were cultured in 89% F12K medium (cat. no. LA1320; Beijing Solarbio Science & Technology Co., Ltd.) supplemented with 10% heat-inactivated fetal bovine serum (cat. no. A511-001; Lonsera; Shanghai Shuangru Biotechnology Co., Ltd.) and 1% penicillin-streptomycin (cat. no. BL505A; Biosharp Life Sciences) at 37˚C with 5% CO_2. The growth of the cells was observed for 24 h and when the cell density reached >80%, they were passaged. SV-HUC-1 cells were used at passages 2 and 3. Cells were authenticated by short tandem repeat profiling and tested negative for mycoplasma contamination. According to previous studies, the stimulatory effect of Ket on cells is both concentration- and time-dependent (20,21). Based on these previous KIC-related studies, the present study selected 0.5, 1, 1.5 and 2 mM as test concentrations for Ket treatment. To test the effects of differing Ket concentrations, SV-HUC-1 cells were initially incubated in 6-well plates. Upon reaching 80% confluency, cells were exposed to equal volumes of Ket at different working concentrations (0, 0.5, 1, 1.5 and 2 mM) for 48 h at 37˚C. Ket hydrochloride was purchased from Fujian Gutian Pharmaceutical Co., Ltd. After 48 h of incubation with Ket, cells were collected for ALDH2 protein semi-quantitative analysis using western blotting.

Transfection of cells for ALDH2 knockdown and overexpression. SV-HUC-1 cells were transfected with siRNA sequences targeting ALDH2 (si-ALDH2) in order to establish a model of ALDH2 knockdown; cells were also transfected with an appropriate non-targeting negative control (NC) siRNA (si-NC). All siRNA sequences used in this study are listed in Table I. The siRNA sequences used were designed and synthesized by Jiangsu Saisuofei Biotechnology Co., Ltd. siRNA sequences were transfected into SV-HUC-1 cells using Lipo8000™ Transfection Reagent (cat. no. C0533; Beyotime Biotechnology) according to the manufacturers' instructions. Reverse transcription-quantitative PCR (RT-qPCR) was used to screen for knockdown efficiency of small interfering RNA (siRNA) sequences. The siRNA sequence with the highest knockdown efficiency was identified to be si-ALDH2-1272 (Figs. S1-S5).

To induce ALDH2 overexpression (OE-ALDH2), the coding DNA sequence (CDs) region of the ALDH2 mRNA sequence was cloned and inserted into the pcDNA3.1-EGFP (Genecefe Bio) overexpression vector. Empty plasmid was used as the NC. PCR conditions: Incubation at 42˚C for 40 min, heating at 85˚C for 5 min and storing at 4˚C. cDNA was stored at -20˚C. The overexpression vector containing the ALDH2 CDs sequence was transfected into SV-HUC-1 cells using Lipo8000 Transfection Reagent (cat. no. C0533; Beyotime Biotechnology) according to the manufacturers' instructions.

The present study subsequently used western blotting to detect the protein expression of ALDH2 in transfected cells to verify the successful transfection of si-ALDH2 and OE-ALDH2 compared with their control groups (Fig. S6). According to the results of the aforementioned investigation into the effects of Ket dosage on ALDH2 expression, 1 mM Ket was selected as the optimal concentration for treatment of SV-HUC-1 cells. Additionally, 10 uM of the mTOR activator MHY1485 (Act; cat. no. HY-B0795; MedChemExpress) was used to treat cells; this helps cells resist apoptosis and oxidative stress damage, allowing them to survive in harsh environments. Subsequently, the present study established a number of treatment groups, including: i) NC groups comprising cells that did not undergo transfection (NC, NC + Act, NC + Ket and NC + Ket + Act groups); ii) ALDH2 knockdown groups (si-ALDH2, si-ALDH2 + Act, si-ALDH2 + Ket and si-ALDH2 + Ket + Act groups); and iii) ALDH2 overexpression groups (OE-ALDH2, OE-ALDH2 + Act, OE-ALDH2 + Ket and OE-ALDH2 + Ket + Act groups). After transfection, cells in each group were incubated with equal volumes of complete culture medium for 48 h at 37˚C before observation under a light microscope and collection for subsequent experiments.

RT-qPCR screening for si-ALDH2 sequence knockdown efficiency. The mRNA sequence of ALDH2 was obtained from the Reference Sequence database curated by the National Center for Biotechnology Information (22) and the primers used in RT-qPCR were designed and synthesized by Sangon Biotech Co., Ltd., using the Primer Premier 5.0 software (Premier Biosoft Inc.). The housekeeping gene GAPDH was used as an internal reference.

Total RNA was extracted from SV-HUC-1 cells using Trizol reagent (cat. no. R1100; Beijing Solarbio Technology Co., Ltd.). Subsequently, 50% by volume chloroform (cat. no. C2432; Merck KGaA) was added to cells for the RNA extraction, and the upper aqueous phase was collected after centrifugation. An equal volume of isopropanol (cat. no. W292907; Merck KGaA) was added to the supernatant before RNA was precipitated by centrifugation at 11,300 x g for 15 min at 4˚C. Extracted RNA was washed with 70% alcohol, dried and suspended in enzyme water. Subsequently, RNA concentration and purity were determined using an ultra-micronucleic acid detector (cat. no. FC-1100; Hangzhou Suizhen Biotechnology Co., Ltd.). A total of 200 ng RNA was reverse transcribed using a reverse transcription kit (cat. no. RN05004M; Mona Biotechnology, Co., Ltd.) according to the manufacturer's protocol, and the resulting cDNA was stored at -20˚C until subsequent use in the qPCR protocol.

First, RNA concentration was measured, followed by cDNA synthesis. Each reaction for the qPCR process included: 5 μl SYBR-Green Premix Taq (cat. no. RN04006M; Mona), 1 μl cDNA (100 ng/μl), 0.3 μl forward primer (10 μmol/l),

Table I. siRNA sequences.

Oligo name	Sequence (5'-3')	RNA concentration, ng/μl
ALDH2-human-1272		260.85
Forward	CCUGAAGUUCAAGACCAUATT	
Reverse	UAUGGUCUUGAACUUCAGGTT	
ALDH2-human-1500		245.37
Forward	GGCAUACACUGAAGUGAAATT	
Reverse	UUUCACUUCAGUGUAUGCCTT	
ALDH2-human-493		250.71
Forward	GGAGACUUCUUCAGCUACATT	
Reverse	UGUAGCUGAAGAAGUCUCCTT	
siRNA FAM marker negative control		263.19
Forward	UUCUCCGAACGUGUCACGUTT	
Reverse	ACGUGACACGUUCGGAGAATT	

0.3 μl reverse primer (10 μmol/l) and 3.4 μl water. The thermocycling conditions were as follows: Initial denaturation was performed at 95˚C for 30 sec, followed by 40 cycles of denaturation at 95˚C for 5 sec, annealing at 60˚C for 30 sec and extension at 72˚C for 15 sec. qPCR was performed on the ABI 7500 qPCR instrument (Thermo Fisher Scientific, Inc.). Relative protein expression was normalized against the expression of GAPDH from control group cells. Protein expression levels were analyzed using SPSS software (Version 23.0; IBM Corp.) via the $2^{-\Delta\Delta Cq}$ method (23). The formulas used for semi-quantification of protein expression were as follows: ΔCq=(Cq gene-Cq GAPDH) and $\Delta\Delta$Cq=(ΔCq treatment-ΔCq control). Primer sequences are provided in Table II.

Table II. Reverse transcription-quantitative PCR primer sequences.

Primer	Sequence (5'-3')	Sequence length, bp
ALDH2		135
Forward	AACCTGTGGGGGTGTGCGG	
Reverse	GGGCGGTGAGGGGTGTCTG	
GAPDH		151
Forward	CGGATTTGGTCGTATTG	
Reverse	GAAGATGGTGATGGGATT	

ALDH2, aldehyde dehydrogenase 2. Primer sequences were designed based on the human ALDH2 mRNA reference sequence (RefSeq accession number NM_000690.4) retrieved from the NCBI Reference Sequence database (https://www.ncbi.nlm.nih.gov) (22).

Cell Counting Kit-8 (CCK-8) determination. After transfection, the cytotoxicity of Ket in SV-HUC-1 cells was evaluated via CCK-8 assay (cat. no. M006; Zhejiang Meisen Cell Technology Co., Ltd.). A total of 20 μl CCK-8 solution was added to each well and cells were incubated with CCK-8 reagent for 2.5 h at 37˚C with 5% CO_2. The absorbance of cells was determined at 450 nm by microplate reader.

Flow cytometry detection of cell apoptosis. After digestion for 2 min with EDTA-free trypsin at room temperature, cells were collected by centrifugation at 25 x g for 5 min at room temperature. Subsequently, cells were resuspended in PBS (cat. no. F002; Zhejiang Meisen Cell Technology Co., Ltd) that had been pre-chilled at 4˚C, centrifuged again as in the first step and washed. Cells were resuspended in 300 μl binding buffer and incubated with 5 μl annexin V-FITC (cat. no. 401006; BestBio) at room temperature for 15 min in the dark. Cells were subsequently stained with 10 μl PI (cat. no. C1052; Beyotime Biotechnology), mixed and incubated in the dark at room temperature for 10 min. Finally, cells were detected by flow cytometry (FACSVerse; BD Biosciences) and analyzed using FlowJo software (version 7.6, BD Biosciences).

Fluorescent probe detection of intracellular reactive oxygen species (ROS) levels. The fluorescent probe 2',7'-dichlorofluorescein diacetate (DCFH-DA) from the Reactive Oxygen Species Assay Kit (cat. no. S0033S; Beyotime Biotechnology) was diluted in serum-free medium to reach a final concentration of 10 μmol/l at a dilution of 1:1,000. The cell culture medium was removed from cell samples of all transfection treatments and cells were subsequently seeded in 12-well plates. A total of 1 ml diluted DCFH-DA was added to each 12-well plate and cells were incubated with the probes at 37˚C for 20 min. Excess DCFH-DA was removed by washing the cells with serum-free cell culture thrice. DAPI was diluted in serum-free culture medium and cells were incubated with DAPI at 37˚C for 10 min. Cells were washed three times with serum-free culture medium and subsequently seeded in complete culture medium. Finally, cells were observed and imaged using a fluorescence microscope (Olympus Corporation). The average fluorescence intensity of ROS was detected using Image J software (National Institutes of Health).

Western blot analysis. Transfected and untransfected cell samples were lysed in RIPA buffer (cat. no. P0013B; Beyotime Biotechnology) containing protease inhibitors (cat. no. S1873;

Beyotime Biotechnology) and the protein concentration was subsequently quantified using the BCA method. Equal amounts of protein (25 μg) were loaded and separated on 12% gels by SDS-PAGE and then transferred onto PVDF membranes (cat. no. IPVH00010; MilliporeSigma). The membranes were rinsed three times with TBST (0.1% Tween-20) for 5 min each time, and then slowly shaken with 5% BSA (cat. no. P0023B; Beyotime Biotechnology) at room temperature for 2 h. After blocking, the membranes were incubated with primary antibodies at 4˚C overnight, washed with TBST (0.1% Tween-20) and subsequently incubated with secondary antibodies at 37˚C for 1 h. The primary antibodies used were as follows: ALDH2 (1:1,000; cat. no. 18818; CST Biological Reagents Co., Ltd.), caspase-3 (1:1,000; cat. no. 9662; CST Biological Reagents Co., Ltd.), nuclear factor erythroid 2-related factor 2 (Nrf2; 1:1,000; cat. no. 12721; CST Biological Reagents Co., Ltd.), mTOR (1:1,000; cat. no. AF6308; Affinity Biosciences), phosphorylated (p)-mTOR (1:1,000; cat. no. AF3308; Affinity Biosciences), cyclooxygenase-2 (COX-2; 1:1,000; cat. no. 12282; CST Biological Reagents Co., Ltd.), NF-κB (1:1,000; cat. no. 12540; CST Biological Reagents Co., Ltd.), p-NF-κB (1:800; cat. no. 3033; CST Biological Reagents Co., Ltd.), IL-1 (1:2,000; cat. no. ab283818; Abcam), IL-6 (1:2,000; cat. no. ab229381; Abcam) and GAPDH (1:5,000; cat. no. 2118; CST Biological Reagents Co., Ltd.). Goat anti-rabbit HRP-conjugated antibodies were used as secondary antibodies (1:10,000; cat. no. AP307P; MilliporeSigma). GAPDH was used as an internal loading control for densitometric analysis, whereas phosphorylated proteins were normalized to their total protein counterparts. ECL luminescent liquid (cat. no. P0018AS; Beyotime Biotechnology) was added to the membrane, and the protein bands on the membrane were visualized. The bands were semi-quantified using MD ImageQuant software (version 5.2; Molecular Dynamics, Inc.).

Co-immunoprecipitation (CO-IP) verification of the protein interaction between mTOR and NF-κB. Cells were lysed in 2 ml of IP lysis buffer [150 mM NaCl, 50 mM Tris (pH 7.5), 1 mM EDTA, 0.5%NP40, 10% glycerol and protease inhibitor cocktail] supplemented with protease inhibitors. The lysates were cleared by centrifugation at 12,000 x g for 15 min at 4˚C. The supernatant was used as the total protein, and a portion was reserved as an input control. Equal amounts of protein (25 μg) were taken and then incubated with 2 μg of rabbit IgG (cat. no. 2729; CST Biological Reagents Co., Ltd.) or 50 μl of anti-mTOR (1:1,00; cat. no. 2983; CST Biological Reagents Co., Ltd.) antibody overnight at 4˚C with gentle agitation. Following this, 50 μl of Protein A/G magnetic beads (cat. no. P2108; Beyotime Biotechnology) were added and incubated for 2 h at 4˚C. The beads were washed three times with lysis buffer at 1,000 x g for 1 min at 4˚C, and the immunoprecipitated proteins were eluted by boiling in SDS loading buffer and subjected to SDS-PAGE followed by immunoblotting (mTOR and NF-κB antibodies, as described in in the western blot analysis).

Statistical analysis. All statistical analyses in the present study were conducted on GraphPad software (version 8.0; Dotmatics) and data are presented as the mean ± SD. Comparisons between groups were performed using one-way ANOVA followed by Tukey's post hoc test. $P<0.05$ was considered to indicate a statistically significant difference. All experiments were repeated independently at least three times to obtain three biological replicates, with triplicate technical replicates performed for each sample.

Results

ALDH2 protein expression in SV-HUC-1 cells. Relative ALDH2 expression levels in the 0.5, 1 and 1.5 mM induction groups were significantly higher compared with the 0 mM control group ($P<0.05$). However, no significant difference in ALDH2 expression was observed in the 2 mM induction group compared with the 0 mM group ($P>0.05$), as shown in Fig. 1. The results of the present study revealed that ALDH2 expression level increased following Ket stimulation; however, ALDH2 expression decreased at Ket concentrations >1.5 mM due to significant reductions in cell viability. Furthermore, caspase-3 protein expression increased as Ket concentration, and therefore SV-HUC-1 cell apoptosis, increased. Caspase-3 protein expression was shown to be Ket concentration-dependent. CCK-8 cell viability assays demonstrated that cell viability steadily decreased with increasing Ket concentration. Based on these experimental results, 1 mM was selected as the optimal working concentration of Ket for subsequent experiments.

ALDH2 protects bladder cells from apoptotic damage. To explore differences in bladder endothelial cell viability under different treatment conditions, the present study ascertained cell viability in NC, ALDH2 knockdown and OE-ALDH2 groups; these groups were subdivided into additional treatment groups comprising cells administered Ket, Act and combination treatments, as well as control groups that were administered no additional treatments. The results of the present study identified that cells in the si-ALDH2 + Ket group demonstrated a notable decrease in cell viability levels compared with the si-ALDH2 group. Similarly, cell viability rates were notably lower in the si-ALDH2 + Ket group compared with the NC + Ket group. Following treatment with Act, cell viability rates markedly increased across all groups. However, the present study observed an increase in cell viability in the OE-ALDH2 + Ket group compared with the NC + Ket group. This increase was notably more pronounced following the addition of Act between si-ALDH2 + Ket and si-ALDH2 + Ket + Act (Fig. 2). There was little difference in cell viability between the NC, si-ALDH2 and OE-ALDH2 groups. Summarily, these results indicated that ALDH2 expression was likely associated with maintaining cell viability in Ket-stimulated SV-HUC-1 cells. Furthermore, the addition of an mTOR activator was shown mitigate the effects of Ket on cell viability.

ALDH2 upregulation reduces cell injury. To further clarify the effects of ALDH2 expression on KIC, the present study used flow cytometry to detect apoptosis in bladder epithelial cells. The results of the present study revealed a significant increase in apoptosis in the si-ALDH2 + Ket group compared with the si-ALDH2 group (Fig. 3). The increase in apoptotic rate observed in the si-ALDH2 + Ket group was also significant compared with the NC + Ket group, which indicated that

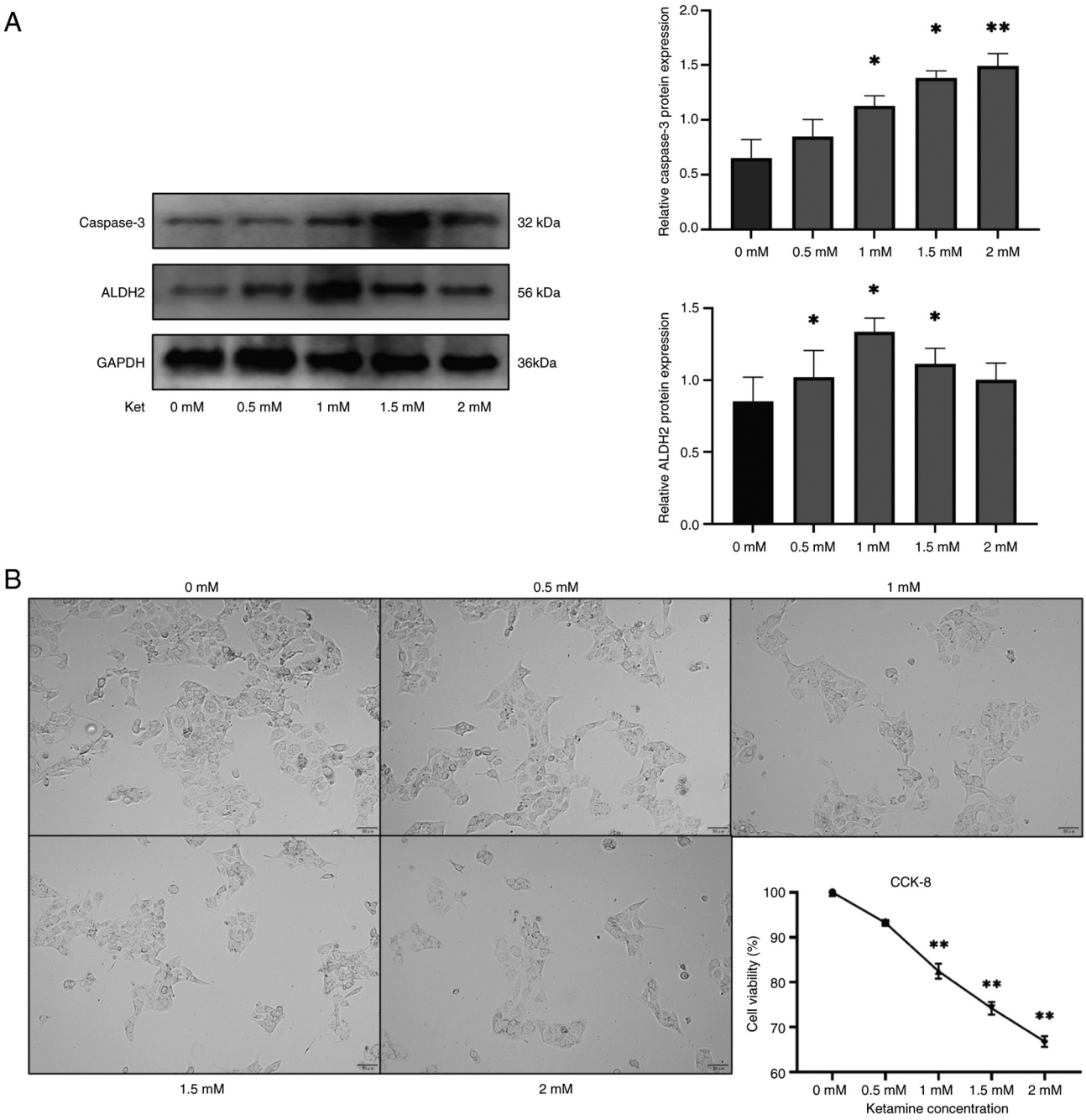

Figure 1. Western blotting and cell viability. (A) Western blotting was used to determine ALDH2 and caspase-3 protein expression in SV-HUC-1 cells that had been treated with different concentrations of Ket (0, 0.5, 1, 1.5 and 2 mM) for 48 h. (B) Cell viability in SV-HUC-1 cells following treatment with various concentrations of Ket. The results of western blot analyses were then semi-quantified. Cell viability at various Ket concentrations was determined via CCK-8 assay. Representative images of SV-HUC-1 cells under various Ket treatments are shown (x100 magnification). Data are expressed as the mean ± SD of 3 biological replicates. *P<0.05 and **P<0.01 vs. 0 mM group. ALDH2, aldehyde dehydrogenase 2; CCK-8, Cell Counting Kit-8; Ket, ketamine.

ALDH2 knockdown promoted apoptosis in KIC. However, apoptotic rate was significantly reduced in the OE-ALDH2 + Ket group compared with the NC + Ket group. This indicated that ALDH2 upregulation may have reduced the occurrence of cell injury. Furthermore, apoptosis appeared to be partially suppressed in bladder cells following co-treatment with Act. These findings suggested that ALDH2 upregulation inhibited apoptosis in bladder endothelial cells.

ALDH2 upregulation mitigates oxidative stress. Apoptosis is largely associated with intracellular oxidative stress (24). Therefore, the present study used fluorescent probes to detect the intracellular ROS levels of various treatment groups. As indicated in Fig. 4, the fluorescence intensity of ROS in the si-ALDH2 + Ket group was significantly greater than in the NC + Ket and si-ALDH2 groups. However, after the addition of Act, the fluorescence intensity of ROS decreased significantly. Furthermore, the fluorescence intensity of ROS in the OE-ALDH2 + Ket group was markedly lower than in the si-ALDH2 + Ket and NC + Ket groups. Furthermore, no significant differences were observed in ROS fluorescence intensity between the NC, NC-Act, si-ALDH2, si-ALDH2 +

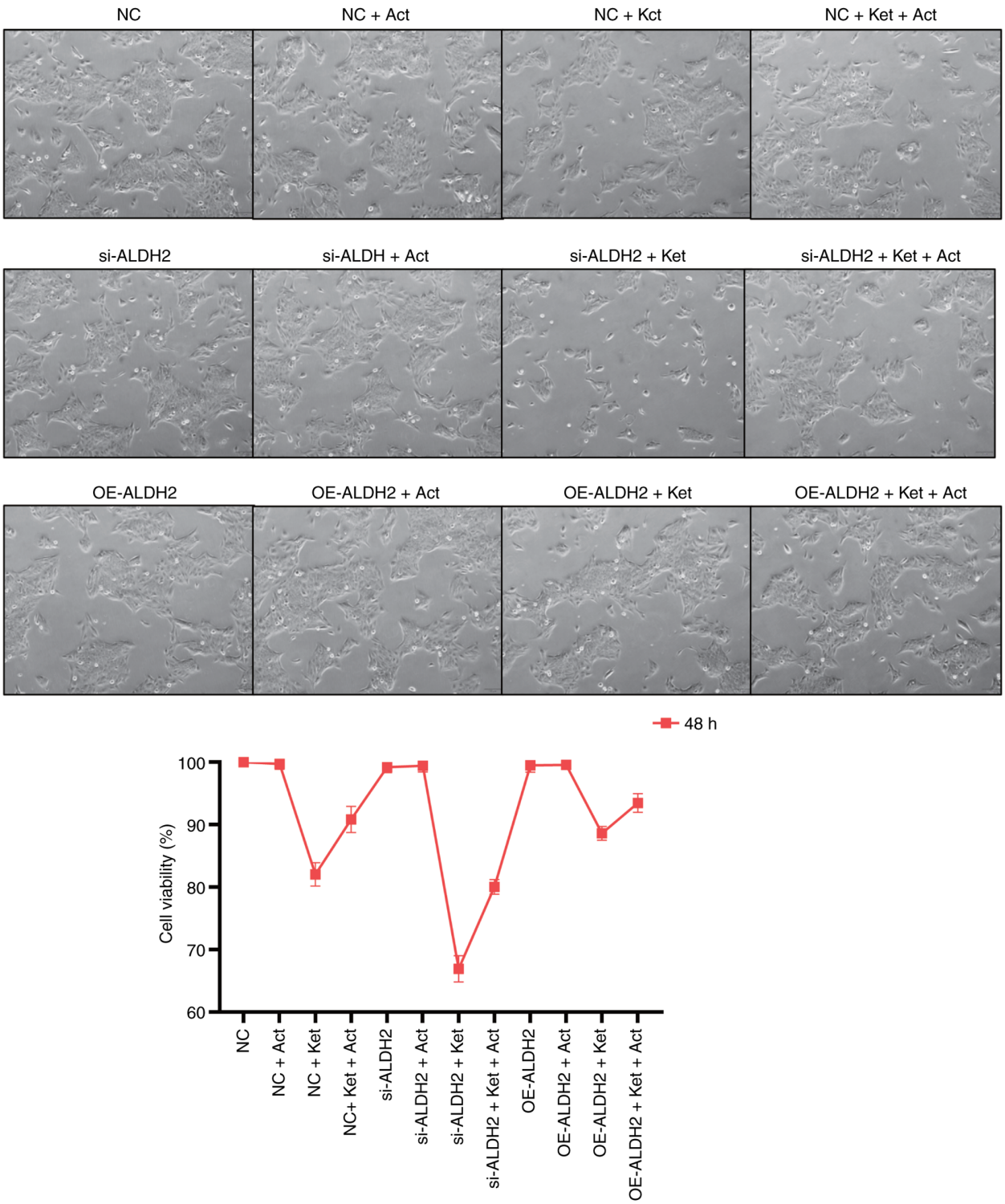

Figure 2. Effects of ALDH2 expression on cell viability in Ket-induced SV-HUC-1 cells. The cell viability of SV-HUC-1 cells was determined by Cell Counting Kit-8 assay. Cells were divided into NC, si-ALDH2 and OE-ALDH2 transfection groups and independently incubated in control, Ket, Act or Ket + Act conditions. Representative images are provided for each group after 48 h of treatment (x100 magnification). Data in the cell viability graph are expressed as the mean ± SD of three biological replicates. NC, negative control; ALDH2, aldehyde dehydrogenase 2; Act, mTOR activator MHY1485; Ket, ketamine; si-ALDH2, small interfering RNA sequences targeting ALDH2; OE-ALDH2, ALDH2 overexpression.

Act, OE-ALDH2 and OE-ALDH2 + Act groups. These findings suggested that ALDH2 upregulation reduced oxidative stress damage in bladder endothelial cells

ALDH2 upregulation prevents inflammation by regulating the mTOR/NF-κB pathway. To further explore the mechanism by which ALDH2 reduces inflammation in the bladder, the present study analyzed the expression of components of the mTOR/NF-κB signaling pathway to elucidate the specific role of ALDH2. Consistent with the results of apoptosis and ROS analyses, the results of western blot analysis (Fig. 5) demonstrated that phosphorylation levels of the nuclear

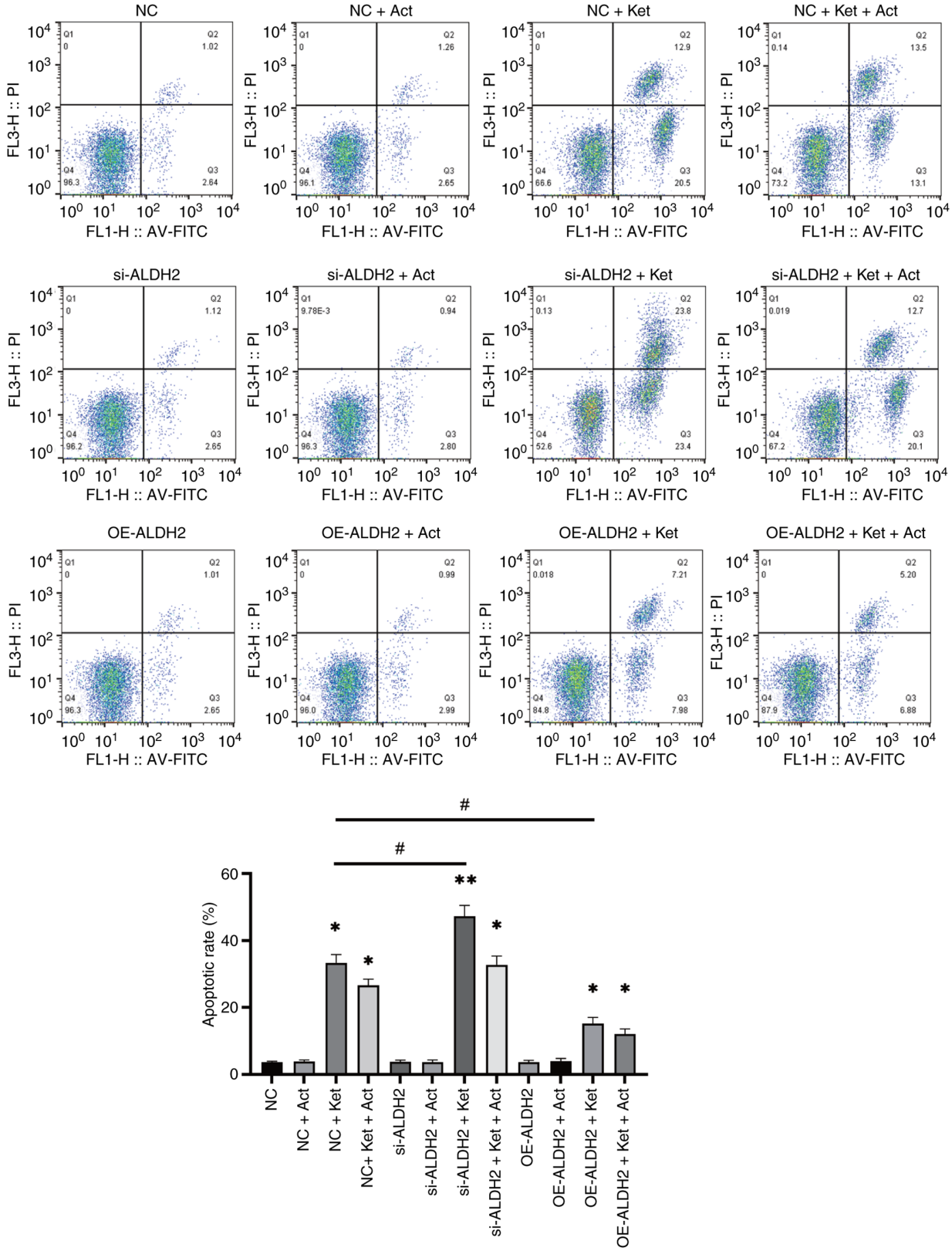

Figure 3. Effects of ALDH2 expression on apoptosis in Ket-induced SV-HUC-1 cells. Apoptosis in various NC, si-ALDH2 and OE-ALDH2 groups was determined by flow cytometry. *P<0.05 and **P<0.01 vs. NC group; $^{\#}$P<0.05 vs. NC + Ket group. Data are expressed as the mean ± SD of 3 biological replicates. NC, negative control; ALDH2, aldehyde dehydrogenase 2; Act, mTOR activator MHY1485; Ket, ketamine; si-ALDH2, small interfering RNA sequences targeting ALDH2; OE-ALDH2, ALDH2 overexpression.

transcription factor NF-κB were highest in the si-ALDH2 + Ket group at a relative expression level of 1.69±0.06; this was significantly higher than the relative expression of p-NF-κB observed in the NC + Ket group at 1.39±0.07. However, this expression was notably reduced in the OE-ALDH2 + Ket group 1.05±0.07. These results show that decreased ALDH2

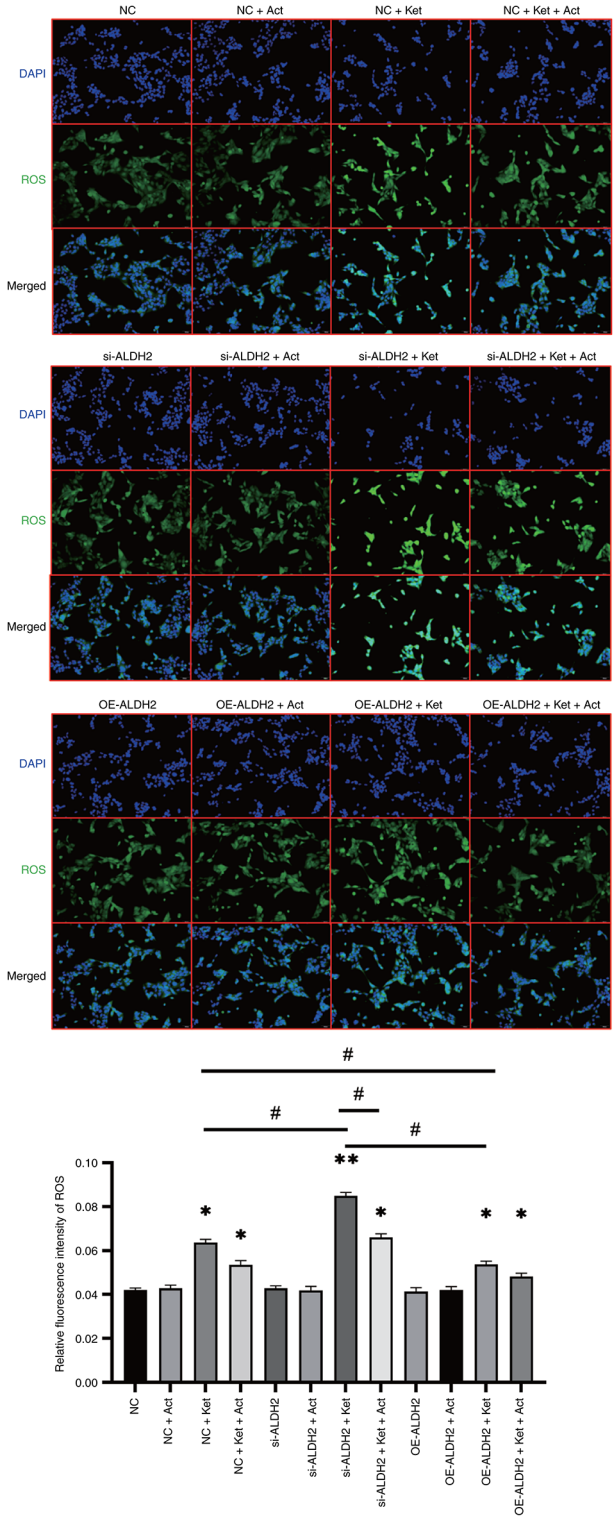

Figure 4. Effects of ALDH2 expression on oxidative stress in Ket-induced SV-HUC-1 cells. Fluorescent probes were used to detect intracellular ROS and fluorescence intensity for each group was quantified and compared (x100 magnification). *P<0.05 and **P<0.01 vs. NC group; $^{\#}$P<0.05 vs. NC + Ket group. Data are expressed as the mean ± SD of 3 biological replicates. NC, negative control; ALDH2, aldehyde dehydrogenase 2; Act, mTOR activator MHY1485; Ket, ketamine; si-ALDH2, small interfering RNA sequences targeting ALDH2; OE-ALDH2, ALDH2 overexpression; ROS, reactive oxygen species.

expression leads to increased inflammation, while upregulation of ALDH2 expression leads to decreased inflammation. It indicates that inflammatory levels were negatively associated with ALDH2 expression. The expression levels of COX-2 (3.51±0.48 vs. 2.48±0.29), IL-1 (4.00±037 vs. 3.29±033) and IL-6 (5.23±0.82 vs. 2.99±0.11) were also significantly elevated in the si-ALDH2 + Ket group compared with the NC + Ket group. Additionally, compared with all other treatment groups in the present study, the si-ALDH2 + Ket treatment group demonstrated the highest expression levels of these proteins, which are all located downstream of NF-κB (25). However, the expression levels of the aforementioned proteins were significantly reduced in the OE-ALDH2 + Ket group compared with the si-ALDH2 + Ket and NC + Ket groups. After co-treatment with Act, the expression levels of the inflammatory proteins COX-2, IL-1 and IL-6 in each transfection group notably decreased. Furthermore, mTOR phosphorylation in the OE-ALDH2 + Ket group was significantly elevated compared with the NC + Ket group. mTOR phosphorylation levels were also significantly lower in the si-ALDH2 + Ket group compared with the NC + Ket group. Nrf2 protein expression showed a similar trend. Compared with the NC + Ket group, significantly reduced expression levels of Nrf2 were observed in the si-ALDH2 + Ket group, which demonstrated the lowest Nrf2 expression levels among all treatment groups. Additionally, significant upregulation of Nrf2 was observed in the OE-ALDH2 + Ket group compared with the NC + Ket group, while, there were no statistical significances between cells not treated with Ket (NC, NC + Act, si-ALDH2, si-ALDH2 + Act, OE-ALDH2 and OE-ALDH2 + Act). These results suggested that ALDH2 may have modulated the degree of inflammation in bladder epithelial cells by promoting mTOR phosphorylation and inhibiting NF-κB expression. Additionally, the results of the CO-IP assay in the present study indicated an indirect or functional interaction between mTOR and NF-κB (Fig. S7).

Discussion

Currently, symptomatic methods remain the primary approach for treating KIC, including steroidal and non-steroidal anti-inflammatory drugs, oral anticholinergics and intravesical instillations of drugs, such as hyaluronic acid. However, the outcomes of such treatments are often poor for patients with late stage KIC, underscoring the notable importance of studying KIC pathogenesis (26). A previous study has reported that bladder urothelial denudation, lamina propria fibrosis and inflammation are common pathological features of KIC (27). Ket and its metabolites in urine exert direct toxic effects on the bladder urothelium, generating free radicals of ROS and reactive nitrogen species. These free radicals react with polyunsaturated fatty acids in the cell membrane to form lipid peroxides, which damage bladder cells and disrupt the bladder mucosal barrier. These lipid peroxides include 4-hydroxy-2-nonenal and malondialdehyde, which can disrupt the mitochondrial respiratory chain and the activity of mitochondrial antioxidant enzymes. Consequently, oxidative stress is considered to be an important factor in the occurrence and development of KIC (17).

ALDH2 can convert aldehydes into their corresponding non-toxic acid forms (28), as well as reduce inflammation and inhibit apoptosis. A study reported by Zhang and Fu (29) revealed that ALDH2 inhibited tumor occurrence

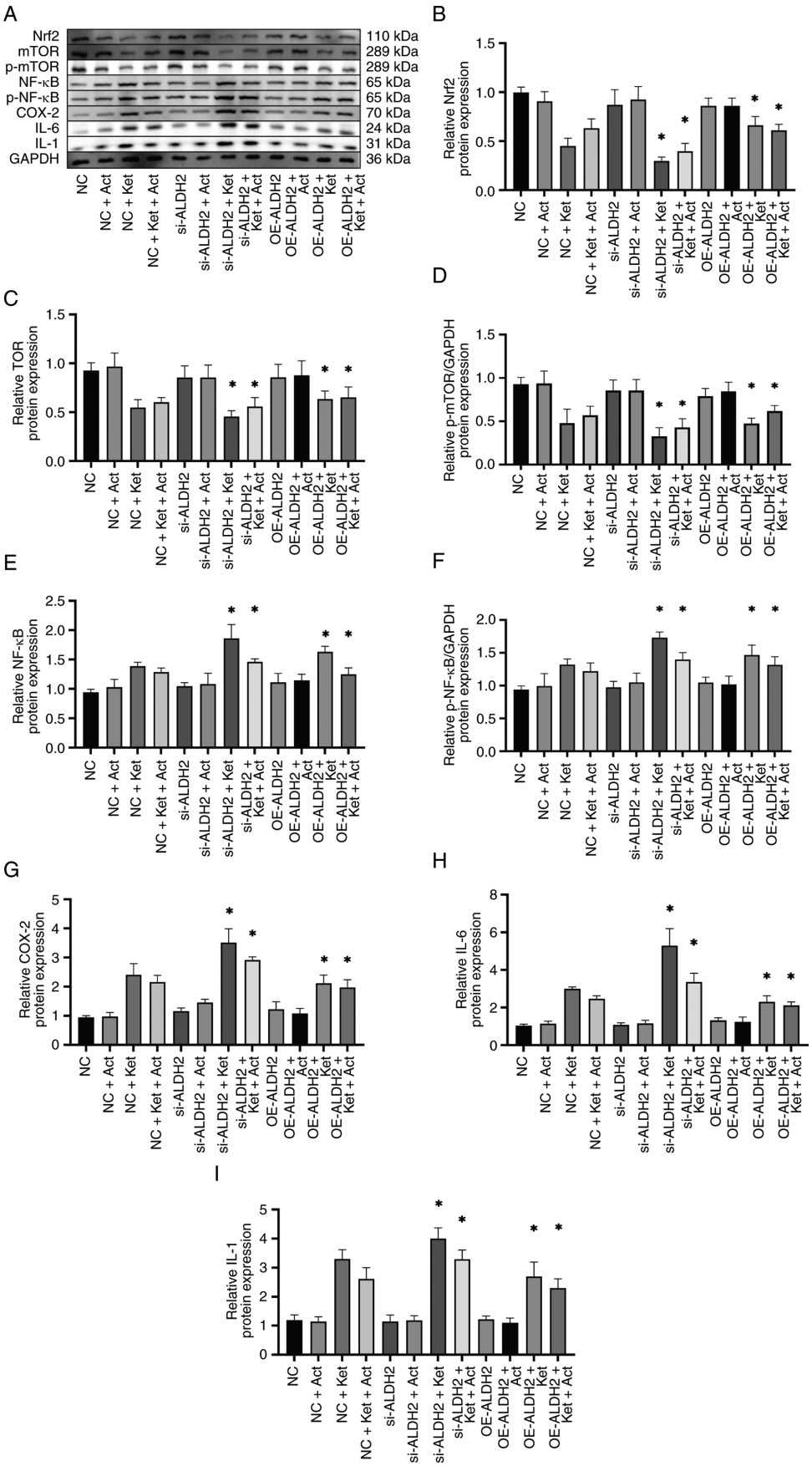

Figure 5. Effects of ALDH2 expression on inflammation in Ket-induced SV-HUC-1 cells. (A) Western blotting was used to detect the protein expression levels and its semi-quantification of (B) Nrf2, (C) mTOR, (D) p-mTOR, (E) NF-κB, (F) p-NF-κB, (G) COX-2, (H) IL-6 and (I) IL-1 in each treatment group. Blots were normalized against GAPDH, with p-mTOR and p-NF-κB expression also normalized against total mTOR and NF-κB. Results of western blotting were semi-quantified. *P<0.05 vs. NC + Ket group. Data are expressed as the mean ± SD of 3 biological replicates. NC, negative control; ALDH2, aldehyde dehydrogenase 2; Act, mTOR activator MHY1485; Ket, ketamine; si-ALDH2, small interfering RNA sequences targeting ALDH2; OE-ALDH2, ALDH2 overexpression; Nrf2, nuclear factor erythroid 2-related factor 2; p-, phosphorylated-; COX-2, cyclooxygenase-2.

and progression, reduced the production of carcinogenic aldehydes and served as a potential target for tumor treatment. Another study by Zhong *et al* (30) also observed that increased ALDH2 expression reduced oxidative stress damage during ischemia-reperfusion injury and inhibited renal cell apoptosis. Furthermore, a study reported by Ramakrishnan *et al* (31) also observed that ALDH2 was upregulated in muscle-invasive bladder cancer as part of a protective anticancer response. Based on the notable antioxidant and anti-inflammatory effects of ALDH2 in urinary tract tumors (16) and inflammation, the aforementioned findings suggest that ALDH2 may represent a novel target for the prevention and treatment of KIC.

The results of our previous *in vivo* study (17) in Ket-induced mice demonstrated that inflammation and fibrosis in ALDH2 knockout mice were markedly increased compared with wild-type mice. To further support our previous hypothesis that ALDH2 exerts protective effects against bladder injury, the present study established a model of Ket-induced bladder endothelial cell injury to study the effects of ALDH2 gene expression on markers of KIC. The present study observed that exposure to low concentrations of Ket upregulated ALDH2 protein expression in SV-HUC-1 cells, which was consistent with our previous *in vivo* observations on ALDH2 expression in mice, indicating that this upregulation might be protective. However, at higher concentrations of Ket, cell damage exceeds its own compensatory capacity, leading to a decrease in the protective expression of ALDH2. With the decrease in ALDH2 expression, apoptosis protein Caspase-3 was further activated and cell viability decreased significantly, demonstrating that ALDH2 may play a role in protecting against oxidative stress. Other studies, such as a study by Ji *et al* (32) on a mouse model of heart failure, identified that heat shock factor protein 1 regulated ALDH2 expression and delayed the onset of heart failure. Furthermore, another study reported by Wohlfart *et al* (33) identified that ALDH2 was upregulated in glyoxalase $1^{-/-}$ zebrafish in a compensatory manner, therefore increasing the antioxidant and detoxification capacity of reactive carbonyl substances.

Upon direct stimulation of bladder mucosal tissue by toxic products, oxidative stress-induced damage results in cellular production of several ROS. Oxidative stress can activate the important inflammatory transcription factor NF-κB. NF-κB, as an upstream core transcription factor, mediates the activation of the caspase cascade further promoting the expression of inflammatory proteins (COX-2 and inducible nitric oxide synthase) and the release of inflammatory mediators (IL-1β and IL-6), and inhibiting the expression of the anti-oxidative protein Nrf2 (34). A study reported by Tsai *et al* (35) observed that ALDH2 transcriptional activation reduced ROS production and inhibited the NF-κB pathway, thereby reducing vascular smooth muscle cell apoptosis and preventing the formation of abdominal aortic aneurysms. Another study revealed that ALDH2 protects the kidneys against ischemia-reperfusion injury by inhibiting the IκBα/NF-κB/IL-17C pathway (36). The experimental results of the present study revealed that in oxidative stress damage induced by Ket, ALDH2 overexpression reduced ROS production and inhibited activation of the NF-κB pathway, reducing the production of inflammatory factors. However, ALDH2 knockdown resulted in an imbalance in oxidation-antioxidant levels, such as increased ROS levels and decreased cell viability, thus activating the NF-κB pathway and increasing the production of pro-inflammatory and pro-fibrotic factors.

mTOR is a serine/threonine kinase that regulates various cellular functions, including the cellular stress response, metabolism, survival and growth (37). Research has increasingly focused on the role of mTOR in a number of important pathophysiological processes in the human body, including inflammation, injury, proliferation, tissue repair and tumorigenesis (38). A study reported by Zahid *et al* (39) on alcohol-induced metabolic diseases demonstrated that transcriptional inhibition of ALDH2 expression resulted in alcohol-induced chronic oxidative stress to modulate the mTOR pathway, thus promoting the onset and progression of hepatocellular carcinoma. Another study has revealed that ALDH2 regulates autophagy via the Akt/mTOR pathway, thereby reducing oxidative stress and mitigating renal ischemia-reperfusion injury (40). The present study demonstrated that in oxidative stress damage induced by Ket, ALDH2 knockdown induced ROS accumulation, which inhibited mTOR via the oxidative stress pathway. Reduced mTOR expression has been shown to impair cellular antioxidant and metabolic homeostasis, which ultimately amplifies the inflammatory and fibrotic responses. Functional interception of ROS activity via methods such as mTOR activation can partially reverse this pathological process (41). Notably, the results of the co-IP assay performed in the present study demonstrated that mTOR and NF-κB are likely associated through functional interactions or indirect pathways, rather than via direct protein-protein interactions.

The results of the present study supported our hypothesis that ALDH2 was likely responsible for reducing the oxidative stress-induced damage to bladder tissue caused by Ket and its metabolites, and that this mitigation of oxidative stress was achieved via regulation of the NF-κB and mTOR pathways to reduce bladder epithelial cell inflammation. Knockdown of the *ALDH2* gene was also shown to aggravate KIC. As these results were consistent with the results of our previous *in vivo* study in mice, we hypothesize that ALDH2 deficiency represents an important risk factor for KIC and other lower urinary tract diseases. Currently, our research into the effects of ALDH2 on KIC has focused on the use of mouse and cell models; however, in future studies we will conduct clinical analyses on patients with KIC, including measurements of daily Ket dosage, and serum and urinary Ket concentration.

Acknowledgements

Not applicable.

Funding

The present work was supported by the Jiangsu University Medical Education Collaborative Innovation Fund (grant no. JDYY2023139) and the Wuxi Municipal Health Commission Scientific Research Youth Project Fund (grant no. Q202462).

Availability of data and materials

The data generated in the present study may be requested from the corresponding author.

Authors' contributions

XX, YY and MZ designed the study, performed experiments, analyzed data and drafted the manuscript. PG contributed towards performing experiments. MZ was also involved in revising the manuscript critically for important intellectual content and giving final approval of the version to be published. Furthermore, MZ was responsible for experimental platforms, funding and laboratory conditions. XX and MZ confirm the authenticity of all the raw data. All authors have read and approved the final version of the manuscript.

Ethics approval and consent to participate

Not applicable.

Patient consent for publication

Not applicable.

Competing interests

The authors declare that they have no competing interests.

References

1. Wang JW, Kivovich V and Gordon L: Ketamine abuse syndrome: Hepatobiliary and urinary pathology among adolescents in flushing, NY. Pediatr Emerg Care 33: e24-e26, 2017.
2. Ezquerra-Romano I, Lawn W, Krupitsky E and Morgan CJA: Ketamine for the treatment of addiction: Evidence and potential mechanisms. Neuropharmacology 142: 72-82, 2018.
3. Orhurhu VJ, Vashisht R, Claus LE and Cohen SP: Ketamine Toxicity. In: StatPerals [Internet]: StatPearls Publishing, Treasure Island, FL, 2025.
4. Jalil R and Gupta S: Illicit ketamine and its bladder consequences: Is it irreversible?. BMJ Case Rep 2012: bcr2012007244, 2012.
5. Noorzurani R, Vicknasingam B and Narayanan S: Illicit ketamine induced frequency of micturition in a young Malay woman. Drug Alcohol Rev 29: 334-336, 2010.
6. Juan YS, Lee YL, Long CY, Wong JH, Jang MY, Lu JH, Wu WJ, Huang YS, Chang WC and Chuang SM: Translocation of NF-κB and expression of cyclooxygenase-2 are enhanced by ketamine-induced ulcerative cystitis in rat bladder. Am J Pathol 185: 2269-228, 20155.
7. Kim A, Yu HY, Heo J, Song M, Shin JH, Lim J, Yoon SJ, Kim Y, Lee S, Kim SW, *et al*: Mesenchymal stem cells protect against the tissue fibrosis of ketamine-induced cystitis in rat bladder. Sci Rep 6: 30881, 2016.
8. Li R, Zhao Z, Sun M, Luo J and Xiao Y: ALDH2 gene polymorphism in different types of cancers and its clinical significance. Life Sci 147: 59-66, 2016.
9. Hu JF, Wang HX, Li HH, Hu J, Yu Y and Gao Q: Inhibition of ALDH2 expression aggravates renal injury in a rat sepsis syndrome model. Exp Ther Med 14: 2249-2254, 2017.
10. Peng J, Wang S, Pan X, Wu M, Zhan X, Wang D, Zhu G, Wang W, Tang H, An N and Pei J: Identification of ALDH2 as a novel target for the treatment of acute kidney injury in kidney transplantation based on WGCNA and machine learning algorithms and exploration of its potential mechanism of action using animal experiments. Front Immunol 16: 1536800, 2025.
11. Wimborne HJ, Hu J, Takemoto K, Nguyen NT, Jaeschke H, Lemasters JJ and Zhong Z: Aldehyde dehydrogenase-2 activation decreases acetaminophen hepatotoxicity by prevention of mitochondrial depolarization. Toxicol Appl Pharmacol 396: 114982, 2020.
12. Xia G, Fan F, Liu M, Wang S, Wu J, Shen C, Han S, Wang C, Jia J, Zou Y, *et al*: Aldehyde dehydrogenase 2 deficiency blunts compensatory cardiac hypertrophy through modulating Akt phosphorylation early after transverse aorta constriction in mice. Biochim Biophys Acta 1862: 1587-1593, 2016.
13. Kucuk A, Kabadere S, Tosun M, Koken T, Kinaci MK, Isikli B and Erkasap N: Protective effects of doxycycline in ischemia/reperfusion injury on kidney. J Physiol Biochem 65: 183-191, 2009.
14. Tang S, Huang T, Jing H, Huang Z, Chen H, Fan Y, Zhong J and Zhou J: Aldehyde dehydrogenase-2 acts as a potential genetic target for renal fibrosis. Life Sci 239: 117015, 2019.
15. Wong SY, Woo J, Leung JC and Leung PC: Depressive symptoms and lifestyle factors as risk factors of lower urinary tract symptoms in Southern Chinese men: A prospective study. Aging Male 13: 113-119, 2010.
16. Wu S, Chen J, Dong P, Zhang S, He Y, Sun L, Zhu J, Cheng Y, Li X, Tang A, *et al*: Global gene expression profiling identifies ALDH2, CCNE1 and SMAD3 as potential prognostic markers in upper tract urothelial carcinoma. BMC Cancer 14: 836, 2014.
17. Xi XJ, Chen SH and Mi H: Aldh2 gene reduces oxidative stress in the bladder by regulating the NF-κB pathway in a mouse model of ketamine-induced cystitis. Exp Ther Med 20: 111, 2020.
18. Liu H, Hu Q, Ren K, Wu P, Wang Y and Lv C: ALDH2 mitigates LPS-induced cardiac dysfunction, inflammation, and apoptosis through the cGAS/STING pathway. Mol Med 29: 171, 2023.
19. Xu T, Guo J, Wei M, Wang J, Yang K, Pan C, Pang J, Xue L, Yuan Q, Xue M, *et al*: Aldehyde dehydrogenase 2 protects against acute kidney injury by regulating autophagy via the Beclin-1 pathway. JCI Insight 6: e138183, 2021.
20. Xi XJ, Zeng JJ, Lu Y, Chen SH, Jiang ZW, He PJ and Mi H: Extracellular vesicles enhance oxidative stress through P38/NF-kB pathway in ketamine-induced ulcerative cystitis. J Cell Mol Med 24: 7609-7624, 2020.
21. Shen CH, Wang ST, Lee YR, Liu SY, Li YZ, Wu JD, Chen YJ and Liu YW: Biological effect of ketamine in urothelial cell lines and global gene expression analysis in the bladders of ketamine-injected mice. Mol Med Rep 11: 887-895, 2015.
22. O'Leary NA, Wright MW, Brister JR, Ciufo S, Haddad D, McVeigh R, Rajput B, Robbertse B, Smith-White B, Ako-Adjei D, *et al*: Reference sequence (RefSeq) database at NCBI: Current status, taxonomic expansion, and functional annotation. Nucleic Acids Res 44: D733-D745, 2016.
23. Livak KJ and Schmittgen TD: Analysis of relative gene expression data using real-time quantitative PCR and the 2(-Delta Delta C(T)) method. Methods 25: 402-408, 2001.
24. Üremiş N and Üremiş MM: Oxidative/nitrosative stress, apoptosis, and redox signaling: Key players in neurodegenerative diseases. J Biochem Mol Toxicol 39: e70133, 2025.
25. Lawrence T: The nuclear factor NF-kappaB pathway in inflammation. Cold Spring Harb Perspect Biol 1: a001651, 2009.
26. Zhou J, Scott C, Miab ZR and Lehmann C: Current approaches for the treatment of ketamine-induced cystitis. Neurourol Urodyn 42: 680-689, 2023.
27. Jhang JF, Hsu YH and Kuo HC: Possible pathophysiology of ketamine-related cystitis and associated treatment strategies. Int J Urol 22: 816-825, 2015.
28. Matsumoto A: Fundamental Properties of aldehyde dehydrogenase 2 (ALDH2) and the importance of the ALDH2 polymorphism. Nihon Eiseigaku Zasshi 71: 55-68, 2016 (In Japanese).
29. Zhang H and Fu L: The role of ALDH2 in tumorigenesis and tumor progression: Targeting ALDH2 as a potential cancer treatment. Acta Pharm Sin B 11: 1400-1411, 2021.
30. Zhong Z, Hu Q, Fu Z, Wang R, Xiong Y, Zhang Y, Liu Z, Wang Y and Ye Q: Increased expression of aldehyde dehydrogenase 2 reduces renal cell apoptosis during ischemia/reperfusion injury after hypothermic machine perfusion. Artif Organs 40: 596-603, 2016.
31. Ramakrishnan S, Granger V, Rak M, Hu Q, Attwood K, Aquila L, Krishnan N, Osiecki R, Azabdaftari G, Guru K, *et al*: Inhibition of EZH2 induces NK cell-mediated differentiation and death in muscle-invasive bladder cancer. Cell Death Differ 26: 2100-2114, 2019.
32. Ji E, Jiao T, Shen Y, Xu Y, Sun Y, Cai Z, Zhang Q and Li J: Molecular Mechanism of HSF1-Upregulated ALDH2 by PKC in ameliorating pressure overload-induced heart failure in mice. Biomed Res Int 2020: 3481623, 2020.
33. Wohlfart DP, Lou B, Middel CS, Morgenstern J, Fleming T, Sticht C, Hausser I, Hell R, Hammes HP, Szendrödi J, *et al*: Accumulation of acetaldehyde in aldh2.1(-/-) zebrafish causes increased retinal angiogenesis and impaired glucose metabolism. Redox Biol 50: 102249, 2022.

34. Yeo D, Hwang SJ, Kim WJ, Youn HJ and Lee HJ: The aqueous extract from Artemisia capillaris inhibits acute gastric mucosal injury by inhibition of ROS and NF-kB. Biomed Pharmacother 99: 681-687, 2018.
35. Tsai SH, Hsu LA, Tsai HY, Yeh YH, Lu CY, Chen PC, Wang JC, Chiu YL, Lin CY and Hsu YJ: Aldehyde dehydrogenase 2 protects against abdominal aortic aneurysm formation by reducing reactive oxygen species, vascular inflammation, and apoptosis of vascular smooth muscle cells. FASEB J 34: 9498-9511, 2020.
36. Chen Y, Xiong Y, Luo J, Hu Q, Lan J, Zou Y, Ma Q, Yao H, Liu Z, Zhong Z and Ye Q: Aldehyde dehydrogenase 2 protects the kidney from ischemia-reperfusion injury by suppressing the IκBα/NF-κB/IL-17C pathway. Oxid Med Cell Longev 2023: 2264030, 2023.
37. Marafie SK, Al-Mulla F and Abubaker J: mTOR: Its critical role in metabolic diseases, cancer, and the aging process. Int J Mol Sci 25: 6141, 2024.
38. Omolekan TO, Chamcheu JC, Buerger C and Huang S: PI3K/AKT/mTOR signaling network in human health and diseases. Cells 13: 1500, 2024.
39. Zahid KR, Yao S, Khan ARR, Raza U and Gou D: mTOR/HDAC1 crosstalk mediated suppression of ADH1A and ALDH2 links alcohol metabolism to hepatocellular carcinoma onset and progression in silico. Front Oncol 9: 1000, 2019.
40. Lin D, Xiang T, Qiu Q, Leung J, Xu J, Zhou W, Hu Q, Lan J, Liu Z, Zhong Z, *et al*: Aldehyde dehydrogenase 2 regulates autophagy via the Akt-mTOR pathway to mitigate renal ischemia-reperfusion injury in hypothermic machine perfusion. Life Sci 253: 117705, 2020.
41. Szwed A, Kim E and Jacinto E: Regulation and metabolic functions of mTORC1 and mTORC2. Physiol Rev 101: 1371-1426, 2021.